CHEMISTRY OF MATERIALS

Article

pubs.acs.org/cm

Solvent-Free Nanocomposite Colloidal Fluids with Highly Integrated and Tailored Functionalities: Rheological, Ionic Conduction, and Magneto-Optical Properties

Donghee Kim,[†] Younghoon Kim,[†] and Jinhan Cho*

Department of Chemical & Biological Engineering, Korea University Anam-dong, Seongbuk-gu, Seoul 136-713, South Korea

Supporting Information

ABSTRACT: We introduce a unique and facile strategy for the preparation of solvent-free nanocomposite colloidal fluids that allows accurate control over the integration of functionalities as well as the composition and dimensions of the nanocomposite structure. For the preparation of colloidal fluids with highly integrated functionalities, oleic acid (OA)-stabilized magnetic nanoparticles (i.e., OA-Fe_3O_4 NPs) and CdSe@ZnS quantum dots (QDs) were first synthesized in nonpolar solvent. In this case, OA-QDs dispersed in toluene were successively phase transferred to thiol-functionalized imidazolium-type ionic liquid (IL-SH) media with rheological and ionic conduction properties. After the functional NPs were synthesized, amine-functionalized dendrimers and OA-Fe_3O_4 NPs were alternately deposited onto silica colloids (i.e., SiO_2/(dendrimer/OA-Fe_3O_4)$_n$) using a ligand-exchange-induced LbL-assembly in organic media. Electrostatic LbL-assembled (anionic polyelectrolyte (PE)/cationic IL-SH-QD)$_n$ multilayers were then sequentially adsorbed onto the outermost dendrimer layer of the magnetic colloids. The resulting functional colloidal fluids were devoid of colloidal aggregation and exhibited strong superparamagnetic, fluorescent, rheological, and ionic conduction properties at room temperature. Furthermore, mixtures of photoluminescent colloidal fluids with and without OA-Fe_3O_4 NPs behaved effectively as magneto-optically separable colloidal fluids. Because a variety of inorganic NPs ranging from metal to transition-metal oxides can be easily incorporated into colloidal substrates via LbL-assembly, our approach provides a basis for exploiting and designing functional colloidal fluids with liquidlike behavior at room temperature.

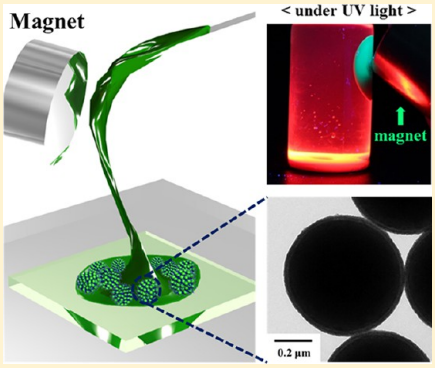

KEYWORDS: *colloids, ionic liquid, nanoparticles, multilayers, layer-by-layer assembly*

INTRODUCTION

Ionic liquids (ILs), which are generally prepared from bulky ionic stabilizers and melt at temperatures less than 100 °C, display great promise in a variety of industrial applications, including catalysis, separations, electrolytes for highly reversible lithium batteries, and phase-change materials for the storage of solar energy. Their utility stems from their unique physicochemical properties such as extremely low vapor pressure, high conductivity, nonflammability, and relatively high thermal and electrochemical stability.[1−6] On the basis of these unique properties, solvent-free nanoparticles (NPs) with liquidlike behavior at room temperature, which are mainly prepared via the grafting IL ligands onto the surface of various inorganic NPs, have recently become attractive candidates for the facile design of novel functional nanomaterials.[7−13]

The physical properties of solvent-free NPs can also be tailored over an unusually broad range through the manipulation of the geometric and chemical characteristics of the NP core and the IL ligands as well as through adjustments to the thermodynamic state variables, such as temperature and volume fraction. As a result, solvent-free NP fluids can be made to exhibit the properties of materials that range from glassy solids to free-flowing liquids through control of the molecular weight and grafting density of the IL on the surface of the NPs. In addition, solvent-free inorganic NP fluids can provide novel routes to functional fluids such as highly conductive lubricating waxes, heat-transfer fluids, or liquid electrolytes for high-temperature electrochemical cells.[9] Although a variety of NP fluids have been synthesized and characterized, the major challenges with developing such NP fluids include the implementation of more than one property at the single-particle level and the facile transformation of physical form, which would allow us to explore novel technological applications. However, to our knowledge, the majority of studies have focused on a single type of NP fluid stabilized by IL ligands. Therefore, the goal of our study was to develop a general method for creating functional fluids that integrate a variety of desired and tailored functionalities into a single particle.

Received: May 13, 2013
Revised: August 5, 2013
Published: September 2, 2013

dx.doi.org/10.1021/cm401560r | *Chem. Mater.* 2013, 25, 3834−3843

Herein, we introduce a versatile and robust approach for the preparation of solvent-free colloidal fluids with highly integrated and adjustable functionalities via layer-by-layer (LbL) assembly.[14−24] LbL assembly is a versatile method that enables the deposition of nanocomposite films with tailored optical, mechanical, or electrical properties onto substrates of various shapes and sizes. For this study, a model system of optical colloidal fluids with superparamagnetic properties was prepared by the ligand-exchange LbL assembly[25,26] of amine-functionalized dendrimers (i.e., poly(amidoamine)) and oleic acid (OA)-stabilized Fe_3O_4 NPs[27] followed by the electrostatic LbL assembly[14−19] of cationic IL-SH-stabilized CdSe@ZnS QDs and oppositely charged polyelectrolytes (PEs). The thiol-functionalized imidazolium-type IL (i.e., IL-SH) layer deposited as an outermost layer on these colloids endowed them with liquidlike behavior at room temperature. In addition, the colloidal fluids exhibited the properties of its component materials (i.e., superparamagnetic, fluorescence, ionic conduction, and rheological properties). Furthermore, we emphasize that these nanocomposite colloidal fluids can be developed into magnetic fluid actuators with reversible optical tuning memory under magnetic control. Although Fe_3O_4 NPs and QDs were used for our model system, we note that other functional NPs, such as Ag and Au, can also be incorporated into the LbL-assembled colloidal fluids. To the best of our knowledge, our article is the first to report the successful preparation of colloidal fluids with complex and integrated functionalities via LbL assembly. Considering that these colloidal fluids can be used as a type of ink for a variety of potential applications such as magneto-optical sensing, magnetically controllable QD display, or magnetically retrievable catalytic colloids, we believe that our approach can provide a basis for designing and synthesizing colloidal fluids with more complex but tailored functionalities.

EXPERIMENTAL SECTION

Materials. Poly(amidoamine) dendrimer (ethylene diamine core type), oleic acid, CdO, zinc acetate, 1-octadecene, selenium, sulfur powder, trioctylphosphine (TOP), tetraoctylammonium bromide (TOABr), poly(allylamine hydrochloride) (PAH), and poly(sodium 4-styrenesufonate) (PSS) were purchased from Sigma-Aldrich. OA-stabilized Fe_3O_4 of about 6 nm and TOABr-stabilized Au NP of about 8 nm were synthesized as previously reported.[27,28]

Synthesis of IL-SH. 1-Methylimidazole (3.09 g, 37.67 mmol) and 3-chloro-1-propanethiol (5 g, 45.20 mmol) were refluxed for 72 h at 80 °C under argon-protected conditions.[29,30]

Synthesis of OA-CdSe@ZnS with Green Emissive Color. OA-stabilized green QDs (PL λ_{max} = 530 nm) were synthesized by a previously reported method.[31] CdO (0.4 mmol) and zinc acetate (8 mmol) were placed with 8 mL of OA in a three-necked flask and heated at 150 °C. After that, 30 mL of 1-octadecene was added in the reaction flask and heated at 300 °C under N_2 conditions. At the elevated temperature (300 °C), 6 mL of TOP dissolving 12 mmol of sulfur powder and 0.3 mmol of Se were rapidly injected into the flask. The reaction proceeded at 300 °C for 10 min. After 10 min, the reaction flask was cooled to room temperature. The obtained QDs were purified repeatedly more than three times using chloroform and an excess amount of acetone followed by dispersion in toluene.

Synthesis of OA-CdSe@ZnS with Red Emissive Color. CdSe@ZnS QDs were synthesized by a previously reported method.[32] CdO (1 mmol) and OA (1 mL) were placed in a three-necked flask and heated at 150 °C. After mixing, 25 mL of 1-octadecene was added in the reaction flask and heated at 300 °C under N_2 conditions. At the elevated temperature (300 °C), 0.4 mL of TOP dissolving 0.4 mmol of Se was rapidly injected into the flask. After 2.5 min of reaction time, 0.13 mL of 1-octanthiol was slowly added. The reaction proceeded at 300 °C for 30 min. After 30 min, the reaction flask was cooled to room temperature. After cooling, 10 mL of 1-ODE dissolving 2 mmol of CdO and 2 mL of OA were injected into the reaction flask and heated at 300 °C under N_2 conditions. At the elevated temperature (300 °C), 0.43 mL of 1-octanthiol was slowly added again. The reaction proceeded at 300 °C for 30 min. After 30 min, the reaction flask was cooled to room temperature. Eight milliliters of OA dissolving 4 mmol of zinc acetate was injected into the flask again and heated at 300 °C under N_2 conditions. At the elevated temperature (300 °C), 2 mL of TBP dissolving 4 mmol of S was rapidly injected. The reaction proceeded at 300 °C for 10 min. After 10 min, the reaction flask was cooled to room temperature. The obtained QDs were purified repeatedly more than three times using chloroform and an excess amount of acetone followed by dispersion in toluene.

Synthesis of IL-SH-CdSe@ZnS and IL-SH-Au NP. For the preparation of IL-SH-CdSe@ZnS or IL-SH-Au NPs, the hydrophobic NPs (i.e., OA-CdSe@ZnS or TOABr-Au NPs) dispersed in toluene solvent were successively phase transferred to IL-SH medium up to the desired NP concentration.

Building of LbL Multilayers. The (dendrimer/OA-Fe_3O_4 NP)$_n$ multilayer-coated SiO_2 colloids were prepared as follows. A concentrated dispersion (6.4 wt %) of anionic 585 nm SiO_2 colloids (100 μL) was diluted to 0.5 mL with deionized water. After centrifugation (8000 rpm, 5 min) of the colloidal solution, the supernatant water was removed and then dendrimer ethanol solution (0.5 mL) of 1 mg mL^{-1} was added to the colloids, which was followed by ultrasonication and sufficient adsorption time. Excess dendrimer was removed by three centrifugation (8000 rpm, 5 min)/wash cycles. Next, 5 mg mL^{-1} OA-Fe_3O_4 NPs/toluene (0.5 mL) was added to prepare multilayers on the dendrimer-coated SiO_2 colloids and the excess OA-Fe_3O_4 NPs were removed after deposition for 10 min by three centrifugation steps as described above. Then, 1 mg mL^{-1} dendrimer/toluene (0.5 mL) (or ethanol) was deposited onto the OA-Fe_3O_4 NP-coated colloids under the same conditions. The above process was repeated until the desired number of layers were deposited on the colloidal SiO_2. Subsequently, electrostatic (IL-SH-CdSe@ZnS or IL-SH-Au NPs/PSS)$_n$ multilayers were deposited onto SiO_2/(dendrimer/OA−Fe_3O_4 NP)$_n$/dendrimer in aqueous solution.

Preparation of Nanocomposite Colloidal Fluids. After centrifugation (8000 rpm, 5 min) of the multilayer-coated colloidal solution (i.e., nanocomposite colloids coated with outermost IL-SH-CdSe@ZnS or IL-SH-Au NPs), the supernatant water was removed and then these colloids were dried at 80 °C overnight under vacuum to remove the residual solvent. For the preparation of the resulting colloidal fluids, IL-SH media was added to the colloids, which was followed by ultrasonication. In this case, the negligible weight loss of about 0.4% was observed in the thermogravimetric analysis of the nanocomposite colloidal fluids (Supporting Information Figure S1).

UV−vis Spectroscopy. UV−vis spectra of dendrimer/hydrophobic NP multilayers on quartz glass were collected with a Perkin-Elmer Lambda 35 UV−vis spectrometer.

Fourier Transform Infrared Spectroscopy (FTIR). Vibrational spectra were measured by FTIR spectroscopy (iS10 FT-IR, Thermo Fisher) in the transmission and attenuated total reflection (ATR) modes. The sample chamber was purged with N_2 gas for 2 h to eliminate water and CO_2 prior to conducting the FTIR measurement. An ATR−FTIR spectrum for the (dendrimer/OA-Fe_3O_4 NP)$_n$ film deposited onto a Au-coated substrate was obtained from 300 scans with an incident angle of 80°. The acquired raw data was plotted after baseline correction, and the spectrum was smoothed using spectrum analyzing software (OMNIC, Nicolet).

Rheological Measurements. Rheological properties, such as shear stress and shear viscosity, were measured using an MCR-301 (Anton Paar) rheometer at 25 °C. Modulus data, including elastic and viscous moduli, were obtained using the same rheometer via a temperature-sweep mode from 25−80 °C with a 10 °C min^{-1} rate under a fixed angular frequency (1 s^{-1}) and strain amplitude (10%).

Magnetic Measurements. Superparamagnetic properties, such as the field dependence of magnetization and reciprocal molar

Scheme 1. Schematic Diagram Showing the Preparation of Solvent-Free Nanocomposite Colloidal Fluids via LbL-Assembled Multilayers

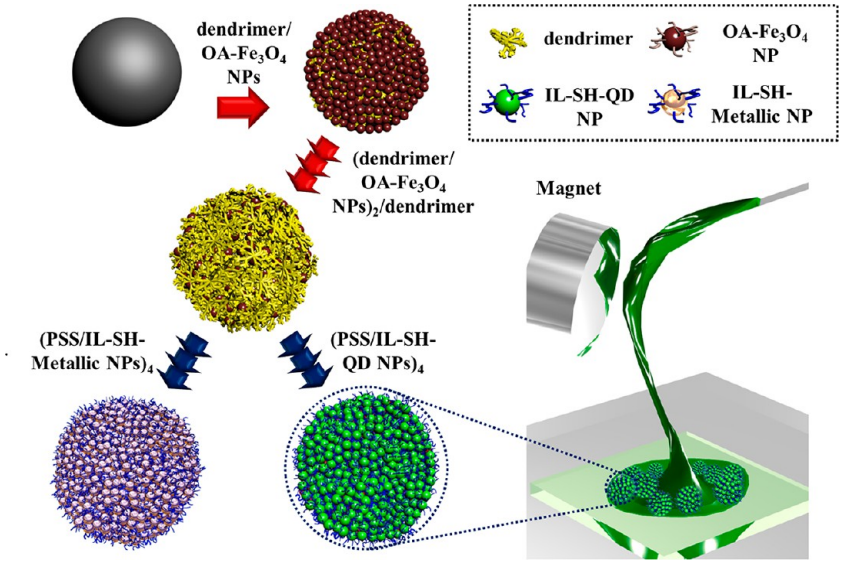

susceptibility, were investigated by a superconducting quantum interference device (SQUID, MPMS5) magnetometer.

RESULTS AND DISCUSSION

In developing solvent-free ILs with highly integrated functionalities, we directed our attention toward nanocomposite colloidal fluids that contain LbL-assembled Fe_3O_4 NPs and fluorescent CdSe@ZnS QDs because of the size-dependent physicochemical properties of NPs and their facile incorporation into colloid surfaces (Scheme 1).

First, 6 nm diameter OA-Fe_3O_4 NPs[27] were directly deposited onto dendrimer-coated silica colloids with a diameter of 600 nm in toluene. The dendrimers were subsequently adsorbed onto the OA-Fe_3O_4 NP layer in ethanol.[19,26] This process was continuously repeated until the desired layer number was achieved. In the ligand-exchange process, the $-COO^-$ group of the OA ligands, which was loosely bound to the surfaces of the Fe_3O_4 NPs, was easily replaced by the dendrimers because of the high affinity between the Fe_3O_4 NPs and the dendrimer amine groups. Successful ligand exchange was confirmed using Fourier transform infrared spectroscopy (FTIR) (Figure 1a). The C−H stretching (2850 and 2927 cm^{-1}) and COO^- stretching[33,34] (1550 and 1640 cm^{-1}) peaks originate from the long aliphatic chains and carboxylic acid groups of the OA ligand, respectively. The N−H stretching (3300 cm^{-1}) peak is attributed to the amine group of the dendrimers, whereas the N−H bending modes at 1550 and 1650 cm^{-1} that arise from the dendrimer nearly overlap with the $-COO^-$ stretching peaks from the OA ligands. We investigated the transmission peak traces (i.e., the C−H stretching of the long aliphatic chains) from the OA ligands in the range of 2850 and 2927 cm^{-1} by alternately depositing dendrimers and OA-Fe_3O_4 NPs onto the substrates. The FTIR spectrum of dendrimer-coated substrate did not contain any notable transmission peaks in the range of 2850 or 2927 cm^{-1}; however, the subsequent deposition of the OA-Fe_3O_4 NP layer produced absorption peaks that arose from the long aliphatic chains of the OA ligands in the investigated wavelength range. The presence of the OA ligands was nearly undetectable after further deposition of the dendrimer layers. In addition, the

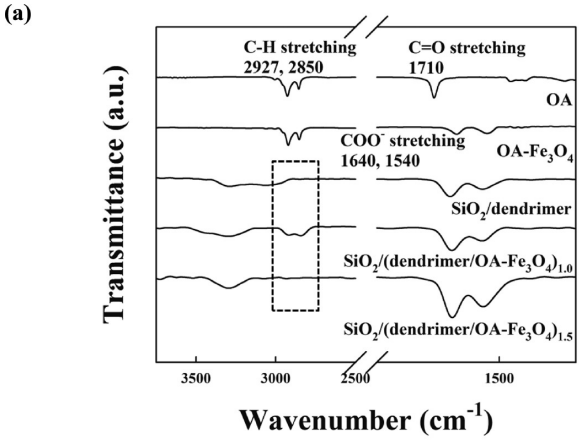

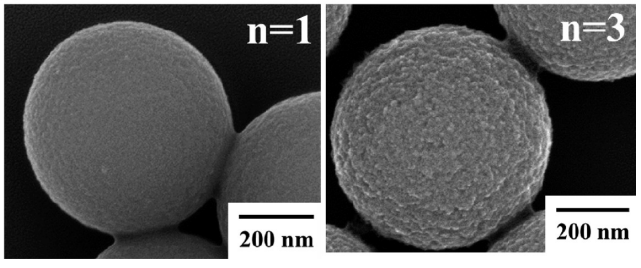

Figure 1. (a) ATR−FTIR spectra of dendrimer, OA, OA-Fe_3O_4, and LbL-assembled $(dendrimer/OA\text{-}Fe_3O_4)_n$ (n = 0.5, 1, and 1.5) multilayers. (b) SEM images of SiO_2 colloids coated with $(dendrimer/OA\text{-}Fe_3O_4\ NP)_n$ (n = 1 and 3).

transmission peaks at 1640 and 1540 cm^{-1} (i.e., the overlapping modes between the N−H bending of the dendrimer and the COO^- stretching of the OA-Fe_3O_4 NPs) gradually intensified as the bilayer number (n) of the $(dendrimer/OA\text{-}Fe_3O_4)_n$ increased from 0.5 to 1.5. This result suggests that the vertical growth of the nanocomposite multilayers occurred via a ligand-exchange reaction between the dendrimers and the OA ligands.

On the basis of these results, dendrimers and Fe_3O_4 NPs were alternately adsorbed onto silica colloids with a diameter of

dx.doi.org/10.1021/cm401560r | Chem. Mater. 2013, 25, 3834−3843

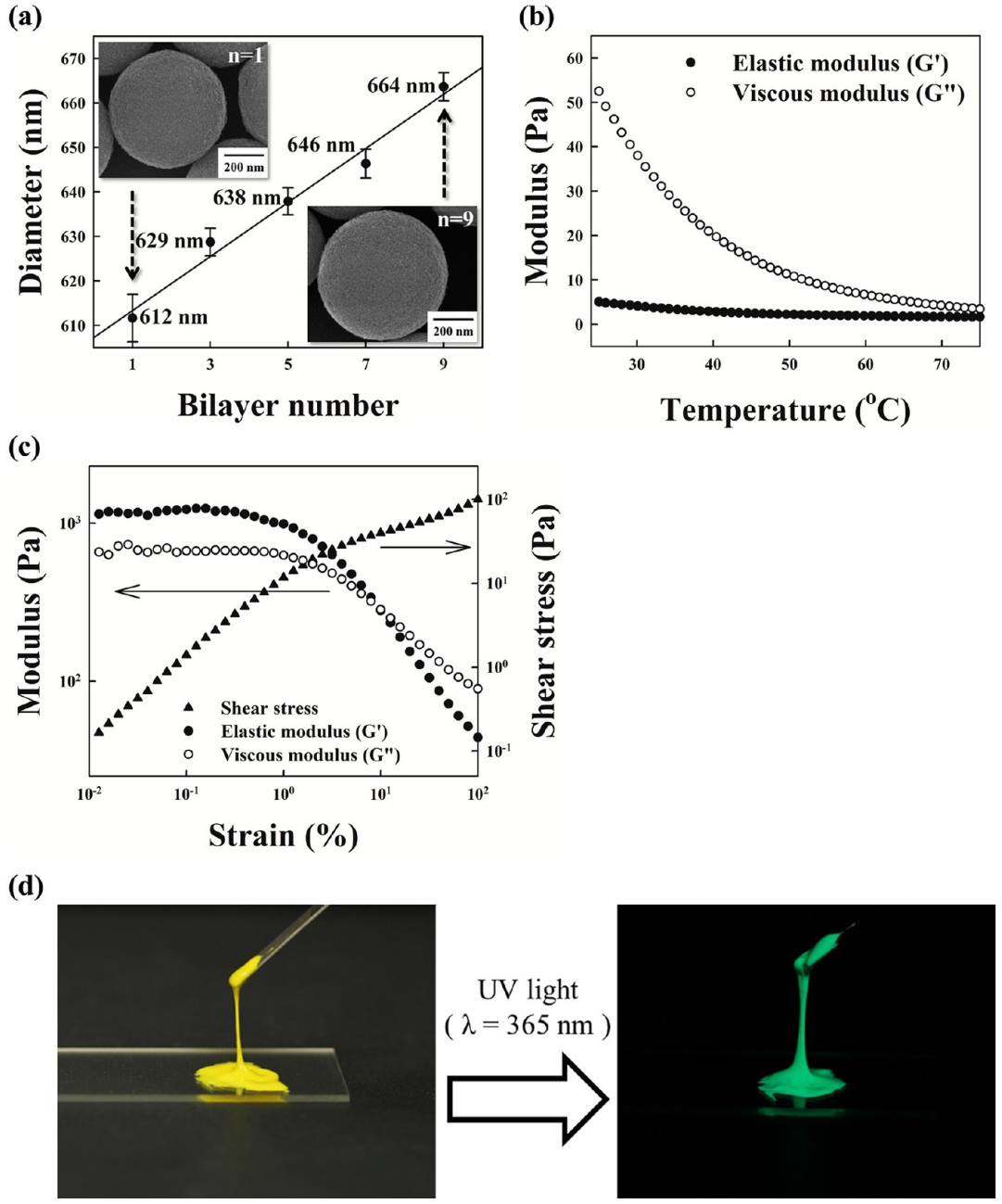

Figure 2. (a) $(PSS/IL\text{-}SH\text{-}CdSe@ZnS)_n$/dendrimer multilayer-coated SiO_2 colloids as a function of bilayer number. The inset shows the cross-sectional scanning electron microscopy (SEM) images of the multilayer-coated colloids. (b) Elastic and viscous modulus as a function of temperature for 33 wt % multilayer-coated colloids. (c) Strain-dependent elastic/viscous moduli (G′/ G″) and shear stress data of the resulting colloidal fluids coated with dendrimer/$(PSS/IL\text{-}SH\text{-}QD_{green})_9$. (d) Photographic image of IL-SH-QD multilayer-based colloidal fluids (33 wt % concentration).

approximately 600 nm in organic media. As shown in Figure 1b, the LbL-assembled dendrimer/OA-Fe_3O_4 NP multilayers were densely and homogeneously deposited onto the silica colloids without any colloidal agglomeration. Notably, for electrostatic LbL-assembled multilayers composed of cationic poly(allylamine hydrochloride) (PAH) and anionic Fe_3O_4 NPs, the amount of anionic Fe_3O_4 NPs adsorbed was relatively low (<30%) because of the strong electrostatic repulsions between NPs of like charge compared to those of OA-Fe_3O_4 NPs deposited in organic media without electrostatic repulsion (Supporting Information Figure S2). Notably, although the ligand-exchange multilayer-coated colloids were prepared through the alternating deposition of OA-Fe_3O_4 NPs in toluene and dendrimers in alcohol, the colloids with an outermost dendrimer layer (i.e., $SiO_2/(dendrimer/OA\text{-}Fe_3O_4\ NP)_n$/dendrimer) were highly miscible in aqueous media (i.e., deionized water with a pH of 5.8). This characteristic arose because of the amine protonation of the dendrimers, which induced electrostatic repulsions between neighboring positively charged colloids in aqueous media and thus prevented colloidal aggregation. Choi and Rubner reported that the pK_a value (i.e., the pH value at which 50% of the functional groups of a polymer are ionized) of an amine-functionalized polymer, such as PAH, is approximately 9.0.[35] Therefore, the protonation of the dendrimers in pH 5.8 water can allow the electrostatic nanocomposite multilayers (i.e., (anionic polyelectrolyte (PE)/

dx.doi.org/10.1021/cm401560r | *Chem. Mater.* 2013, 25, 3834−3843

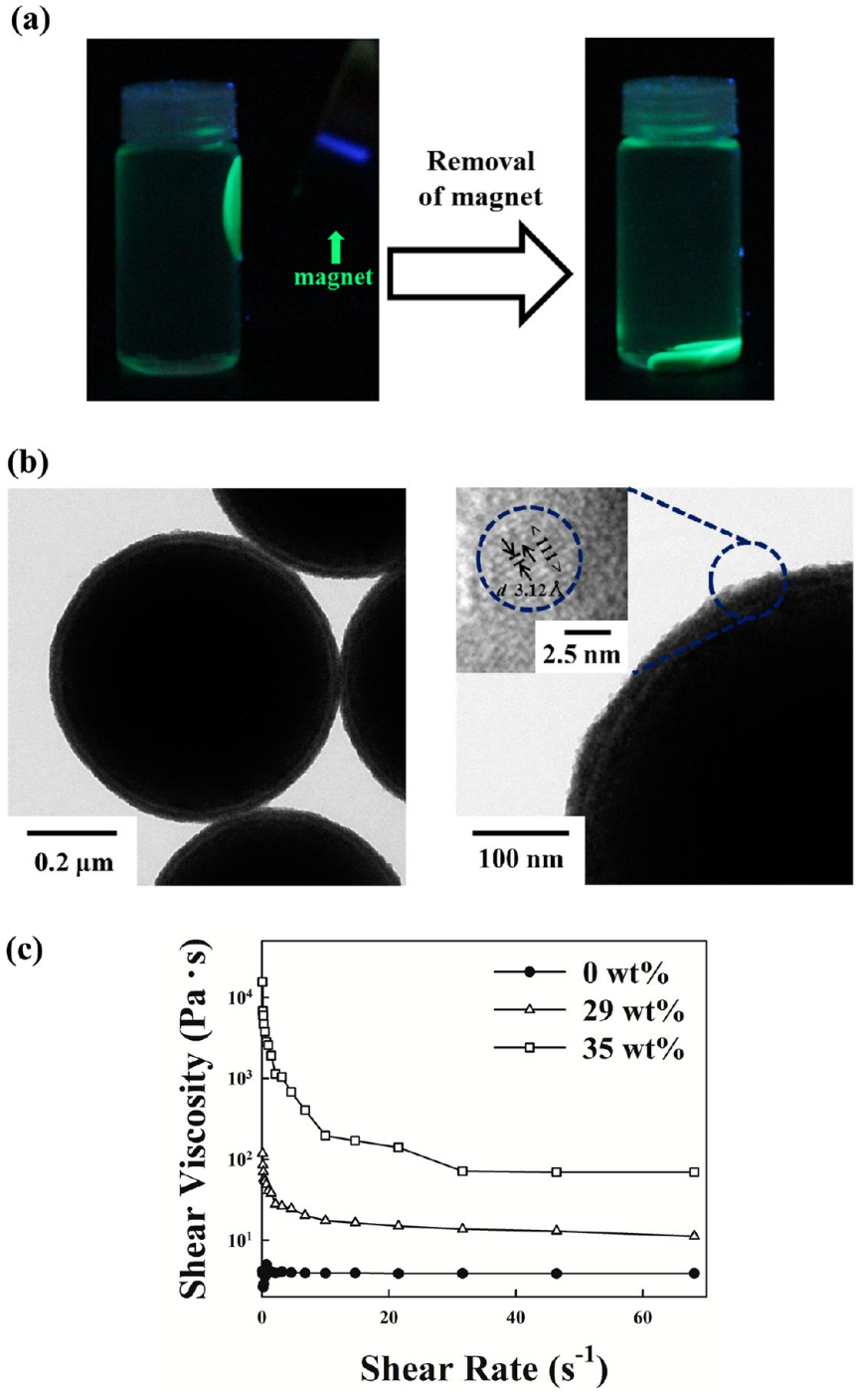

Figure 3. (a) Photographic images of magnetic and photoluminescent multilayer-coated colloidal fluids (60 wt % concentration). The colloidal structure is SiO_2 colloid/(dendrimer/OA-Fe_3O_4)$_3$/dendrimer/(PSS/IL-SH-QD)$_4$. (b) HR-TEM images of SiO_2 colloid/(dendrimer/OA-Fe_3O_4)$_3$/dendrimer/(PSS/IL-SH-QD)$_4$. The inset shows the crystalline structure of outermost IL-SH-CdSe@ZnS NP layer. (c) Shear viscosity data of pure IL-SH and LbL multilayer-coated colloidal fluids with magnetic and fluorescent properties as a function of the shear rate.

cationic NP)$_n$) to be successfully deposited onto the magnetic NP multilayer-coated colloids prepared in organic media.

Encouraged by these advantageous characteristics, we synthesized cationic IL-SH-QD$_{green}$ (i.e., CdSe@ZnS) with green emission and then prepared (anionic PE/cationic IL-SH-QD$_{green}$)$_n$ multilayer-coated silica colloids (Figure 2a). The thiol-functionalized imidazolium-type ILs (i.e., IL-SH) used in our study were first synthesized from 1-methylimidazole and 3-chloro-1-propanethiol.[29,30] For the preparation of IL-SH-QD$_{green}$, the OA-QDs synthesized in hexane were directly phase-transferred to the IL-SH media (see the Experimental Section for details). The IL-SH-QD$_{green}$ dispersed in deionized water were LbL assembled with oppositely charged poly(sodium 4-styrenesulfonate) (PSS) onto dendrimer-modified silica colloids (i.e., SiO_2/dendrimer/(PSS/IL-SH-QD$_{green}$)$_n$). As the bilayer number (n) of the (PSS/IL-SH-QD$_{green}$)$_n$ increased from 1 to 9, the diameter of the colloids increased from 612 to 664 nm. The colloids coated with an outermost layer of IL-SH-QD$_{green}$ were precipitated by centrifugation to remove the aqueous media and were subsequently redispersed in IL-SH

dx.doi.org/10.1021/cm401560r | *Chem. Mater.* 2013, 25, 3834−3843

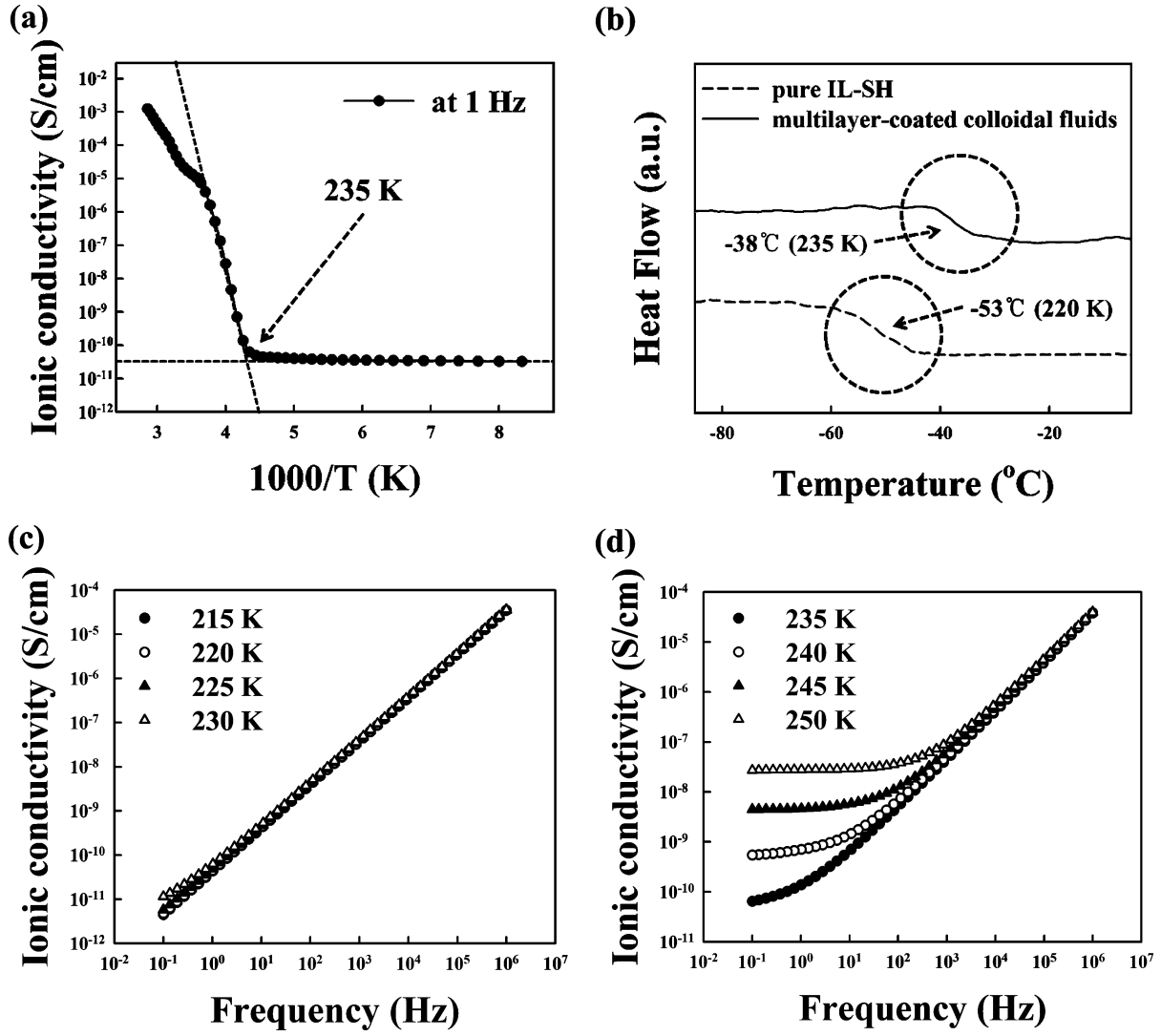

Figure 4. (a) Temperature-dependent ionic conductivity of 29 wt % LbL multilayer-coated colloidal fluids (i.e., SiO_2 colloids/(dendrimer/OA-Fe_3O_4)$_3$/dendrimer/(PSS/IL-SH-QD_{green})$_4$) measured at a fixed frequency of 1 Hz. (b) DSC analysis of pure IL-SH and 29 wt % LbL multilayer-coated colloidal fluids. Frequency-dependent ionic conductivity of IL-SH-containing multilayer-coated colloids at temperatures (c) below and (d) above the glass transition temperature (T_g).

host media. The resulting solvent-free colloidal fluids exhibited typical liquidlike behavior despite a loading of approximately 33 wt % (Supporting Information Figure S3). This behavior was confirmed by rheological measurements, which revealed that the viscous modulus (G″) was substantially higher than the elastic modulus (G′) at temperatures that ranged from 25 to 75 °C (Figure 2b). Recently, it was reported by Archer et al. that self-suspended NP liquid shows soft glassy behavior because of the smaller spacing of the organic chains (i.e., corona chains) than the random-walk step length when the diameter of the NPs is comparable to the organic chain length.[36,37] However, in our system, the IL-SH used as NP ligand and host medium has low molecular weight and short chain length. Therefore, the nanocomposite colloidal fluids do not display the rheological properties of soft glassy materials because the chain length of IL-SH is much smaller than the 6 nm sized CdSe@ZnS QDs as well as the colloidal substrate with a diameter of about 600 nm. For confirming these possibilities, the typical strain-dependent elastic/viscous moduli (G′/ G″) and shear stress were measured from two different samples: (1) solvent-free QD fluids composed of 6 nm sized QD and IL-SH (Supporting Information Figure S4) and (2) nanocomposite colloidal fluids (>600 nm) (Figure 2c). In this case, the resulting colloidal fluids exhibited the simple viscous behavior without the maximum peak of G″,[38] as opposed to the soft glassy behavior with the maximum peak of G″.

These results clearly demonstrate that the fluidic behavior of the IL-SH-colloids (i.e., SiO_2/dendrimer/(PSS/IL-SH-QD_{green})$_9$) originates from the physical properties of the IL-SH used as a ligand in the outermost QD layer as well as from the solvent-free media. Notably, the measured modulus values (G′ and G″) of the IL-SH-nanocomposite colloids were higher than those of pure IL-SH because of the presence of solid colloids (Supporting Information Figure S5). Imidazolium-type ILs, such as IL-SH, have been reported to exist as a 3D network or supramolecular structure of cations and anions linked together by weak interactions (primarily hydrogen bonds).[3−6] Therefore, IL-SH-QD_{green}-encapsulated nanocomposite colloids can effectively participate in a supramolecular structure induced by the IL-SH media without any phase segregation despite the incorporation of relatively large colloids into the IL media. This phenomenon was visually confirmed by photographic images of

dx.doi.org/10.1021/cm401560r | Chem. Mater. 2013, 25, 3834−3843

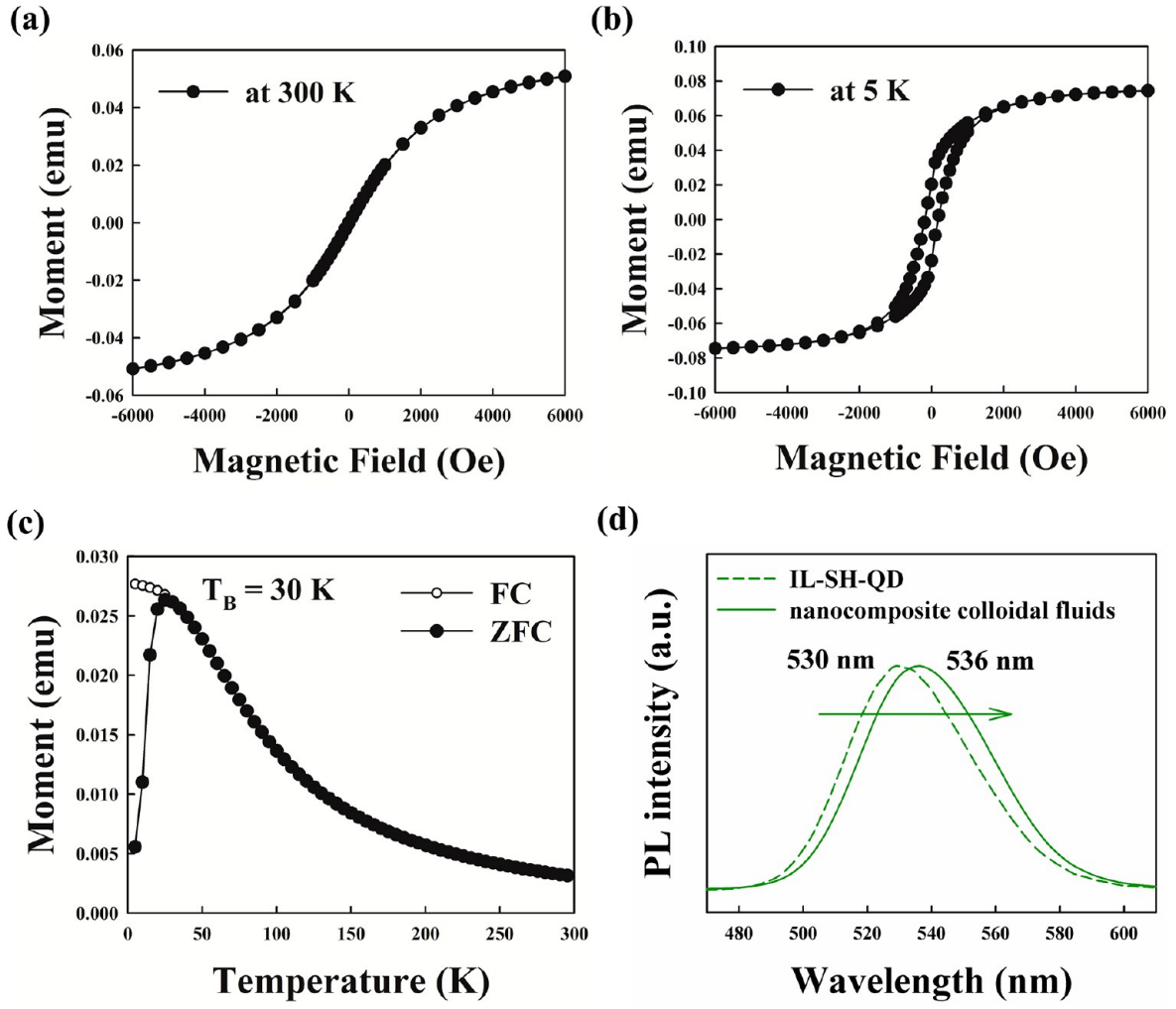

Figure 5. Magnetic curves of magnetic and photoluminescent multilayer-coated colloidal fluids (i.e., SiO_2 colloids/(dendrimer/OA-Fe_3O_4)$_3$/dendrimer/(PSS/IL-SH-QD)$_4$) measured at (a) 300 and (b) 5 K. (c) Temperature dependence of zero-field-cooling (ZFC) and field-cooling (FC) magnetization measured at 150 Oe. (d) Photoluminescent spectra of nanocomposite multilayer-coated colloids ([i.e., SiO_2 colloid/(dendrimer/OA-Fe_3O_4)$_3$/dendrimer/(PSS/IL-SH-QD)$_4$).

the fluorescent colloidal fluids measured at an excitation wavelength of 365 nm (Figure 2c).

Furthermore, we prepared solvent-free multifunctional colloids with magnetic and fluorescent properties using both ligand exchange and electrostatic LbL assembly (Figure 3a). The multilayer structure of these colloids was composed of SiO_2/(dendrimer/OA-Fe_3O_4)$_3$/dendrimer/(PSS/IL-SH-QD_{green})$_4$, and the surfaces of the resulting nanocomposite colloids were highly uniform and homogeneous without any colloidal aggregation (Figure 3b). The inset of Figure 3b indicates the crystalline structure of the outermost IL-SH-CdSe@ZnS NP layer deposited onto multilayer coated colloids. Furthermore, the respective components and crystalline phases of inorganic NPs (i.e., OA-Fe_3O_4 and OA-CdSe@ZnS NPs) embedded within multifunctional colloids (i.e., SiO_2 colloid/(dendrimer/OA-Fe_3O_4)$_3$/dendrimer/(PSS/IL-SH-QD)$_4$) were confirmed by the energy dispersive spectroscopy (EDS) and X-ray diffraction (XRD) analysis (Supporting Information Figure S6). These results suggest that nanocomposite colloids with greater complexity and integrated layer structures that exhibit a high degree of colloidal stability can be easily prepared. In addition, the rheological behavior of the multifunctional colloids exhibited non-Newtonian fluid characteristics in that the shear viscosity increased with increased colloid loading (Supporting Information Figure S7); this behavior can be well explained using a shear-thinning behavior model (Figure 3c).[39,40] These results imply that the insertion of the dendrimer/OA-Fe_3O_4 NP multilayers between the SiO_2 core and the IL-SH-QD_{green}-based multilayers does not significantly affect the overall fluidic behavior of the multifunctional colloids.

We also investigated the temperature-dependent ionic conductivity (σ) of 29 wt % LbL multilayer-coated colloidal fluids (i.e., SiO_2 colloids/(dendrimer/OA-Fe_3O_4)$_3$/dendrimer/(PSS/IL-SH-QD_{green})$_4$), as shown in Figure 4a. The ionic conductivity of the colloidal fluids rapidly increased from 3.27×10^{-11} to 1.23×10^{-3} S cm^{-1} as the temperature was increased from 120 to 350 K, in accordance with the Vogel–Tammann–Fulcher (VTF) model.[41−43] The ionic conductivity plateaued at temperatures below 235 K. This plateau implies that the fluidity of the LbL multilayer-coated colloids in the solid phase does not affect the ionic conductivity. In contrast, the ionic conductivity of the colloidal fluids increased sharply at temperatures greater than 235 K (the point at which the ionic ligands begin to behave as a fluid). Li et al. reported that a decrease in interionic interactions in IL media causes an extreme increase in ionic conductivity.[44] These phenomena

dx.doi.org/10.1021/cm401560r | Chem. Mater. 2013, 25, 3834−3843

were confirmed by an analysis of the differential scanning calorimetry (DSC) traces of the LbL multilayer-coated colloidal fluids during heating. In particular, the glass-transition temperatures (T_g) of pure IL-SH and 29 wt % colloidal fluids were measured to be approximately 220 and 235 K, respectively (Figure 4b). Yoshida et al. reported that T_g behavior is observed instead of melting temperature (T_m) behavior when the alkyl groups in alkyl-methylimidazolium ILs are changed from ethyl to butyl groups.[45] It should be noted that IL-SH used in our study is propyl-methylimidazolium IL. Furthermore, at temperatures below 235 K, the ionic conductivity of the colloidal fluids was strongly influenced by changes in frequency but not by changes in temperature. These phenomena are caused by the formation of a solid phase such that the ionic movement is significantly decreased. The dependence of the ionic conductivity on frequency followed a power law: $\sigma(\omega) \propto \omega^1$ (Figure 4c). In addition, at temperatures higher than 235 K, the ionic conductivity of the colloidal fluids remained constant at low frequencies (i.e., 0.1−10^2 Hz) and, however, gradually increased as the frequency was increased from 10^2 to 10^6 Hz because of the increased mobility of ions (Figure 4d). These results correspond to "universal" dielectric response for many solids including ionic materials and polymers.[46,47]

Remarkably, despite the reduced mobility of the colloidal fluids, the ionic conductivity of the colloidal fluids measured at room temperature was 10−100 times greater than the conductivities of inorganic NP ILs reported by other research groups.[7,8] This phenomenon can be attributed to the high ionic conductivity of IL ligands with a relatively small M_w compared to that of traditional ILs based on bulky organic or polymer ligands.

On the basis of these rheological and ionic conduction properties, the magnetization of the magnetic and fluorescent colloids was examined by superconducting quantum interference device magnetometry (SQUID). The magnetization curves of the colloidal fluids measured at room temperature (300 K) were reversible without coercivity, remanence, or hysteresis, which suggests typical superparamagnetic behavior (Figure 5a).[27,48−50] At liquid helium temperature (5 K), the thermally activated magnetization-flipping properties of the Fe_3O_4 NP layers adsorbed onto the colloids resulted in frustrated superparamagnetic properties (Figure 5b). The magnetization curves acquired a loop shape, with distinct separation of the two sweeping directions, as typically observed with ferromagnets. Figure 5c exhibits the temperature dependence of the magnetization of the multifunctional colloids from 300 to 5 K under an applied magnetic field of 150 Oe. The magnetic anisotropy constant (K), meaning the energy to change the magnetic moment direction of Fe_3O_4 NP, can be expressed using the equation related to the blocking temperature (T_B) as follows: $K = 25\ k_B\ T_B\ V^{-1}$, where k_B is Boltzmann's constant and V is the volume of a single particle. The T_B,[51] which began to deviate slightly between zero-field-cooling (ZFC) and field-cooling (FC) magnetization, was constant at approximately 30 K for the multilayered films.

Park et al. reported that the T_B of 6 nm sized Fe_3O_4 NPs was approximately 30 K. Therefore, our results suggest that the unique magnetic properties of isolated Fe_3O_4 NPs with a diameter of approximately 6 nm can be maintained in multilayer structures. Poddar et al. reported that the T_B of an Fe_3O_4 NP array shifted to significantly higher temperatures upon transitioning from isolated NPs to a 3D NP array because of the relatively strong dipolar interactions between the magnetic moments of individual NPs.[52] In our study, the Langmuir−Blodgett method was used to fabricate Fe_3O_4 NP multilayers without the aid of insulating polymers. However, the dendrimer/OA-Fe_3O_4 NP multilayers in our approach successfully preserved the magnetic properties of isolated Fe_3O_4 NPs because the inserted dendrimer layer effectively screened the dipolar interactions between neighboring Fe_3O_4 NPs.

Figure 5d shows the PL spectrum and photographic images of colloidal fluids. The PL spectrum of multifunctional colloidal fluids with $(PSS/IL\text{-}SH\text{-}QD)_4$ multilayers was slightly shifted relative to that of dilute IL-SH-QD (approximately 5 wt %) with the same PL peak maxima (Supporting Information Figure S8). This red shift in the PL peak results from an exciton energy transfer because of dipole−dipole interactions among neighboring QDs_{green}. In addition, the fluidic behavior of the resulting colloids could be easily controlled with a hand-held magnet. Notably, solvent-free colloids with metal NP shells could be easily prepared using IL-SH-Au NPs instead of IL-SH-QDs (Supporting Information Figure S9).

Furthermore, our approach enabled the production of magneto-optically separable fluids. These "smart" colloidal fluids were prepared by the sequential deposition of IL-SH-QD_{green} and OA-Fe_3O_4 NPs onto silica colloids, thereby producing $SiO_2/(dendrimer/OA\text{-}Fe_3O_4)_3/dendrimer/(PSS/IL\text{-}SH\text{-}QD_{green})_4$. The resulting magnetic luminescent colloidal fluids were mixed with IL-SH-QD_{red}-coated colloidal fluids that lacked OA-Fe_3O_4 NPs (i.e., $SiO_2/(PSS/IL\text{-}SH\text{-}QD_{red})_4$). As depicted in Figure 6, when a hand-held magnet was placed

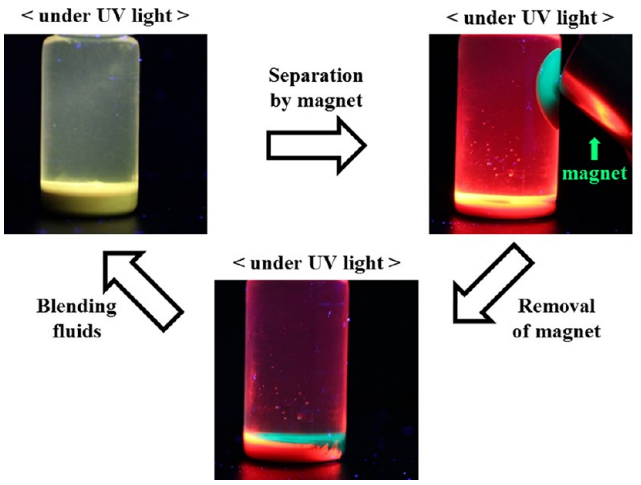

Figure 6. Photographic images of magnetically separable fluids displaying photoluminescent properties. The used fluids were composed of two different kinds of colloids coated with $(dendrimer/OA\text{-}Fe_3O_4)_3/dendrimer/(PSS/IL\text{-}SH\text{-}QD_{green})_4$ and $dendrimer/(PSS/IL\text{-}SH\text{-}QD_{red})_4$ multilayers, respectively.

close to the glass vial, the magnetic photoluminescent fluids that exhibited green emission were quickly attracted to the magnet and accumulated near it within a few minutes. The remaining fluid exhibited red emission, corresponding to the inserted IL-SH-QD_{red}-coated colloids that lack Fe_3O_4 NP layers. These results demonstrate that the blending of photoluminescent colloidal fluids with and without Fe_3O_4 NPs enables reversible, optically tuned properties under magnetic control and furthermore can be effectively applied to develop magnetically controllable actuators with optical

dx.doi.org/10.1021/cm401560r | Chem. Mater. 2013, 25, 3834−3843

switching properties. Considering that a variety of functional materials from biomaterials to metal or metal-oxide particles can be easily incorporated into colloids using traditional LbL assembly, we believe that our approach can play an important role in providing a basis for the synthesis of multifunctional IL fluids.

CONCLUSIONS

We demonstrated that solvent-free colloidal fluids with rheological, magnetic, conductive, and magneto-optical functionalities could be successfully prepared using ligand-exchange- and electrostatic-interaction-based LbL assembly. The ionic conductivity of the colloidal fluids with non-Newtonian fluid behavior significantly increased from 3.27×10^{-11} to 1.23×10^{-3} S cm^{-1} as the temperature was increased from 120 to 350 K. In addition, the outermost layer coatings of IL-SH-QDs onto the silica colloids produced the colloidal fluids with strong fluorescent properties in IL media. We also demonstrated that magnetic and photoluminescent colloids can be used as functional fluids, allowing for a magneto-optical separation or optical switching property. Furthermore, given that a variety of functional materials ranging from biomaterials to metal or metal-oxide NPs can be easily incorporated into colloids using traditional LbL assembly, we believe that our approach can provide a basis for the development and design of solvent-free nanocomposite fluids with more complex and integrated functionalities.

ASSOCIATED CONTENT

Supporting Information

SEM images of multilayer-coated substrates, TGA data of the resulting colloids, shear-strain-dependent elastic/viscous moduli and shear stress data of solvent-free QD fluids, TEM images, UV−vis and PL spectra of nanoparticles, elastic and viscous modulus for pure IL-SH media, EDS and XRD data, and photographic images of nanocomposite colloidal fluids (PDF). This material is available free of charge via the Internet at http://pubs.acs.org.

AUTHOR INFORMATION

Corresponding Author

*E-mail: jinhan71@korea.ac.kr.

Author Contributions

†These authors equally contributed to this work.

Notes

The authors declare no competing financial interest.

ACKNOWLEDGMENTS

This work was supported by the National Research Foundation (NRF) grant funded by the Korea government (MEST) (2010-0029106) and an ERC Program of NRF grant funded by the Korea government (MEST) (R11-2005-048-00000-0).

REFERENCES

(1) Welton, T. *Chem. Rev.* **1999**, *99*, 2071−2084.
(2) Seddon, K. R.; Stark, A.; Torres, M. *Pure Appl. Chem.* **2000**, *72*, 2275−2287.
(3) Dupont, J. *Acc. Chem. Res.* **2011**, *44*, 1223−1231.
(4) Antonietti, M.; Kuang, D.; Smarsly, B.; Zhou, Y. *Angew. Chem., Int. Ed.* **2004**, *43*, 4988−4992.
(5) Dieter, K. M.; Dymek, C. J.; Heimer, N. E.; Rovang, J. W.; Wilkes, J. S. *J. Am. Chem. Soc.* **1988**, *110*, 2722−2726.
(6) Consorti, C. S.; Suarez, P. A. Z.; de Souza, R. F.; Burrow, R. A.; Farrar, D. H.; Lough, A. J.; Loh, W.; da Silva, L. H. M.; Dupont, J. *J. Phys. Chem. B* **2005**, *109*, 4341−4349.
(7) Bourlinos, A. B.; Herrera, R.; Chalkias, N.; Jiang, D. D.; Zhang, Q.; Archer, L. A.; Giannelis, E. P. *Adv. Mater.* **2005**, *17*, 234−237.
(8) Sun, L.; Fang, J.; Reed, J. C.; Estevez, L.; Bartnik, A. C.; Hyun, B.-R.; Wise, F. W.; Malliaras, G. G.; Giannelis, E. P. *Small* **2010**, *6*, 638−641.
(9) Warren, S. C.; Banholzer, M. J.; Slaughter, L. S.; Giannelis, E. P.; DiSalvo, F. J.; Wiesner, U. B. *J. Am. Chem. Soc.* **2006**, *128*, 12074−12075.
(10) Zhou, J.; Tian, D.; Li, H. *J. Mater. Chem.* **2011**, *21*, 8521−8523.
(11) Plechkova, N. V.; Seddon, K. R. *Chem. Soc. Rev.* **2008**, *37*, 123−150.
(12) Moganty, S. S.; Jayaprakash, N.; Nugent, J. L.; Shen, J.; Archer, L. A. *Angew. Chem., Int. Ed.* **2010**, *49*, 9158−9161.
(13) Dupont, J.; Scholten, J. D. *Chem. Soc. Rev.* **2010**, *39*, 1780−1804.
(14) Decher, G. *Science* **1997**, *277*, 1232−1237.
(15) Caruso, F.; Caruso, R. A.; Möhwald, H. *Science* **1998**, *282*, 1111−1114.
(16) Zhai, L.; Cebeci, F. C.; Cohen, R. E.; Rubner, M. F. *Nano Lett.* **2004**, *4*, 1349−1353.
(17) Lee, S. W.; Kim, J.; Chen, S.; Hammond, P. T.; Shao-Horn, Y. *ACS Nano* **2010**, *4*, 3889−3896.
(18) Jiang, C.; Markutsya, S.; Pikus, Y.; Tsukruk, V. V. *Nat. Mater.* **2004**, *3*, 721−728.
(19) Yoon, M.; Choi, J.; Cho, J. *Chem. Mater.* **2013**, 1735−1743.
(20) Lee, B.; Kim, Y.; Lee, S.; Kim, Y. S.; Wang, D.; Cho, J. *Angew. Chem., Int. Ed.* **2010**, *49*, 359−363.
(21) Yoon, M.; Kim, Y.; Cho, J. *ACS Nano* **2011**, *5*, 5417−5426.
(22) Ko, Y.; Kim, Y.; Baek, H.; Cho, J. *ACS Nano* **2011**, *5*, 9918−9926.
(23) Lee, S.; Lee, B.; Kim, B. J.; Park, J.; Yoo, M.; Bae, W. K.; Char, K.; Hawker, C. J.; Bang, J.; Cho, J. *J. Am. Chem. Soc.* **2009**, *131*, 2579−2587.
(24) Cho, J.; Hong, J.; Char, K.; Caruso, F. *J. Am. Chem. Soc.* **2006**, *128*, 9935−9942.
(25) Zhang, F.; Srinivasan, M. P. *Langmuir* **2007**, *23*, 10102−10108.
(26) Ko, Y.; Baek, H.; Kim, Y.; Yoon, M.; Cho, J. *ACS Nano* **2013**, *7*, 143−153.
(27) Sun, S.; Zeng, H.; Robinson, D. B.; Raoux, S.; Rice, P. M.; Wang, S. X.; Li, G. *J. Am. Chem. Soc.* **2004**, *126*, 273−279.
(28) Gittins, D. I.; Caruso, F. *Angew. Chem., Int. Ed.* **2001**, *40*, 3001−3004.
(29) Kim, Y.; Kim, D.; Kwon, I.; Jung, H. W.; Cho, J. *J. Mater. Chem.* **2012**, *22*, 11488−11493.
(30) Kim, Y.; Cho, J. *Nanoscale* **2013**, *5*, 4917−4922.
(31) Bae, W. K.; Char, K.; Hur, H.; Lee, S. *Chem. Mater.* **2008**, *20*, 531−539.
(32) Bae, W. K.; Kwak, J.; Lim, J.; Lee, D.; Nam, M. K.; Char, K.; Lee, C.; Lee, S. *Nano Lett.* **2010**, *10*, 2368−2373.
(33) Sun, S. *Adv. Mater.* **2006**, *18*, 393−403.
(34) Zhang, L.; He, R.; Gu, H.-C. *Appl. Surf. Sci.* **2006**, *253*, 2611−2617.
(35) Choi, J.; Rubner, M. F. *Macromolecules* **2005**, *38*, 116−124.
(36) Agarwal, P.; Qi, H.; Archer, L. A. *Nano Lett.* **2010**, *10*, 111−115.
(37) Agarwal, P.; Srivastava, S.; Archer, L. A. *Phys. Rev. Lett.* **2011**, *107*, 268302-1−268302-5.
(38) Li, Q.; Dong, L.; Fang, J.; Xiong, C. *ACS Nano* **2010**, *4*, 5797−5806.
(39) Hyun, Y. H.; Lim, S. T.; Choi, H. J.; Jhon, M. S. *Macromolecules* **2001**, *34*, 8084−8093.
(40) Felicia, L. J.; Philip, J. *Langmuir* **2013**, *29*, 110−120.
(41) Vogel, H. *Phys. Z.* **1921**, *22*, 645−646.
(42) Tammann, V. G. *Z. Anorg. Allg. Chem.* **1926**, *158*, 1.
(43) Fulcher, G. S. *J. Am. Ceram. Soc.* **1925**, *8*, 339−355.
(44) Li, J.-G.; Hu, Y.-F.; Sun, S.-F.; Ling, S.; Zhang, J.-Z. *J. Phys. Chem. B* **2012**, *116*, 6461−6464.
(45) Yoshida, Y.; Saito, G. *J. Mater. Chem.* **2006**, *16*, 1254−1262.

(46) Jonscher, A. K. *Nature* **1977**, *267*, 673−679.
(47) Jonscher, A. K. *J. Phys. D: Appl. Phys.* **1999**, *32*, R57−R70.
(48) Hong, X.; Li, J.; Wang, M.; Xu, J.; Guo, W.; Li, J.; Bai, Y.; Li, T. *Chem. Mater.* **2004**, *16*, 4022−4027.
(49) Wang, L.; Yang, Z.; Zhang, Y.; Wang, L. *J. Phys. Chem. C.* **2009**, *113*, 3955−3959.
(50) Kim, Y.; Lee, C.; Shim, I.; Wang, D.; Cho, J. *Adv. Mater.* **2010**, *22*, 5140−5144.
(51) Rumpf, K.; Granitzer, P.; Morales, P. M.; Poelt, P.; Reissner, M. *Nanoscale Res. Lett.* **2012**, *7*, 445-1−445-4.
(52) Poddar, P.; Telem-Shafir, T.; Fried, T.; Markovich, G. *Phys. Rev. B* **2002**, *66*, 060403-1−060403-4.